



Analysis of different protocols using an Exradin A12 cylindrical chamber for electron beam reference dosimetry

Prospero^{a,b,c}, G.P.; Ferreira^a, A.C.; Pina^d, D.R.; Pernomian^a, A.C.; Oliveira^a, W.

^a University Hospital of the Botucatu Medical School (HCFMB), UNESP, Department of Radiotherapy, 18618-687, Botucatu, São Paulo, Brazil

^b RTCON Group, São Paulo, São Paulo, Brazil

^c Federal District Base Hospital (HBDF), Department of Radiotherapy, 70330-150, Brasília, Federal District, Brazil

^d University Hospital of the Botucatu Medical School (HCFMB), UNESP, Department of Tropical Diseases and Imaging Diagnosis, 18618-687, Botucatu, São Paulo, Brazil

corresponding author: andregprospero@gmail.com

ABSTRACT

The Technical Report Series 398 (TRS-398), Electron Dosimetry Working Party (EWDP), and Task Group 51 (TG 51) are the most important protocols for reference dosimetry. In the case of electron beam reference dosimetry, these protocols recommend using parallel-plate ionization chambers for beams with R_{50} values below specific thresholds. However, recent papers suggested using cylindrical chambers for reference dosimetry of all electron beam energies. Here we compared different protocols using a cylindrical chamber with the recommendations of using a parallel-plate chamber and the TRS-398 formalism for the dosimetry of several electron beam energies. We employed electron beams with nominal energies of 4, 6, 9, 12, and 15 MeV of a Varian 2100C linear accelerator, an Exradin A12, and an Exradin P11 chamber for the analysis. The results showed differences below 3% when comparing the cylindrical chamber and alternative protocols with the parallel-plate chamber and the TRS-398 formalism for electron beams reference dosimetry. These results can bring confidence in using a cylindrical chamber for reference electron beam dosimetry, which can make the electron beam dosimetry procedure simpler and faster.

Keywords: electron beam, dosimetry, cylindrical chambers, parallel-plate chambers.

1. INTRODUCTION

The protocols for electron beam reference dosimetry, such as Technical Report Series 398 (TRS-398) [1], Task Group 51 (TG 51) [2], and the Electron Dosimetry Working Party (EDWP) [3], were published in nearly two decades ago. Still, these are considered the standard protocols for reference dosimetry and are employed in most radiotherapy departments worldwide.

The standard protocols recommend using parallel-plate ionization chambers for low-energy electron beam reference dosimetry. TRS-398 and EDWP recommend that the parallel-plate chambers must be used for electron beams with half-value depth in water (R_{50} – the depth of water in which the electron beam deposited 50% of its energy) $\leq 4 \text{ g cm}^{-2}$, where their use is preferred in higher-energy beams [1, 3]. TG 51, in its turn, recommends nearly the same, with the mandatory use of parallel-plate chambers for electron beam energies with $R_{50} \leq 2.6 \text{ g cm}^{-2}$ [2]. The main reason for these recommendations is related to early publications that reported significant fluence corrections for cylindrical chambers [4]. These significant fluence corrections would result in considerable uncertainties due to cavity size variations between chambers of the same model (due to the manufacturing process) if general correction factors were employed [5]. Also, it was believed that a well-guarded parallel-plate chamber could minimize the effect of the in-scatter electrons perturbation on the measurements [6]; and the thin front windows of these chambers would allow neglecting the wall influence on the measurements [5].

Although the standard protocols presented reliable results over the last two decades, some issues related to their methodologies and assumptions were addressed in more recent publications. According to the new data reported by Muir and McEwen, the uncertainties associated with the use of cylindrical chambers (NE2571) for all electron beam energies are not worse than for the parallel-plate chambers (NACP-02 and Roos) [5]. A Monte Carlo (MC) simulation study showed that the effects of the in-scatter electron perturbation are present in parallel-plate chambers, even for those with wider guard electrodes [5, 7]. Another study using MC simulations showed significant influences of the parallel-plate chamber's wall in the reference depth (1.7%), which increased beyond the reference depth [8]. Moreover, some authors have questioned the long-term calibration stability of parallel-plate chambers, recommending their cross-calibration each time they are used [9, 10], and

stated that using cylindrical chambers would improve the accuracy of the electron beam calibration procedure and make it simpler [5].

In this way, there is still interest in using Farmer-like cylindrical chambers for the reference dosimetry of all electron beam energies. Indeed, some authors suggest that the standard protocols need to be updated in several ways, one of which is to include the use of cylindrical chambers for dosimetry of all electron beam energies [11]. Using cylindrical chambers for the reference dosimetry of all electron beams would simplify the measurements and make it faster since it would be unnecessary to cross-calibrate the parallel plate against the cylindrical reference chamber nor change the chamber type between photons and electron beam measurements.

We aim to compare different electron beam dosimetry protocols using parallel-plate Exradin P11 and cylindrical Exradin A12 chambers. Other studies employed different ionization chambers and focused on the beam quality correction factors [9, 10], fluence corrections, chamber-to-chamber variations [5], and new formalisms [11]. Here we aim to quantify how much the results obtained using cylindrical chambers associated with different protocols differ from the standard reference protocol (TRS-398 formalism and parallel-plate ionization chambers). The results shown here can bring confidence in using cylindrical chambers for the dosimetry of all electron beam energies if a parallel-plate ionization chamber is unavailable or if the standard protocols are updated to include the use of cylindrical chamber for low-energy electron beams (namely, beams with $R_{50} \leq 2.6 \text{ g cm}^{-2}$ for the TRS-398 protocol, and with $R_{50} \leq 4 \text{ g cm}^{-2}$ for the TG 51 protocol) dosimetry.

2. MATERIALS AND METHODS

We studied the differences between electron beam dosimetry protocols using a parallel plate and cylindrical chambers in this work. We utilized a medical linear accelerator (LINAC) Varian model 2100C of the University Hospital of the Botucatu Medical School (HCFMB) – UNESP radiotherapy department. The LINAC presents electron beams with nominal energies of 4, 6, 9, 12 and 15 MeV (with determined R_{50} of 1.23, 2.33, 3.64, 5.09 and 6.42 g.cm^{-2} , respectively). We also employed an Exradin P11 parallel-plate chamber, an Exradin A12 cylindrical chamber, and a PTW Unidos-E electrometer. The chambers and LINAC have been running in clinical routine for the last two decades,

presenting reliable and traceable data. For the measurements setup, we used a water phantom of $38 \times 38 \times 38 \text{ cm}^3$, a manual positioning system with a precision of a tenth of millimeters, an electron applicator of $15 \times 15 \text{ cm}^2$, and a reference cerrobend block frame of $15 \times 15 \text{ cm}^2$, also routinely employed for clinical dosimetry. We monitored the water-phantom temperature and room pressure during all the beam measurements. Furthermore, we ensured that all beams were in good condition of flatness and symmetry using a PTW QC6 Plus constancy test device.

Firstly, we measured three times ($n = 3$, where n is the number of measurements) the Percentage Depth Dose (PDD) and used the mean values to define the values of R_{50} and reference depth (z_{ref} [mm]) for all electron beams. For the PDD measurements, we employed the P11 parallel-plate chamber, a Source to Surface Distance (SSD) of 100 cm, and 100 Monitor Units (MU) for each depth measurement, as recommended by the standard protocols methodologies [1, 2]. Following this, we proceed to the dosimetry measurements with the P11 parallel plate and A12 cylindrical ionization chambers. When using the P11, the chamber was positioned at the z_{ref} , discounting its front wall (i.e., initially, the chamber emerged 1 mm from the $\text{SSD} = 100 \text{ cm}$) [1, 2]. When using the A12, the measurements were performed with the chamber's central axis positioned at the z_{ref} and at the $z_{\text{ref}} + 0.5r_{\text{cav}}$ (where r_{cav} is the internal radius of the chamber's cavity [mm]), to include all evaluated protocols specifications [1, 2, 11]. All the measurements were carried out using $\text{SSD} = 100 \text{ cm}$, 100 UM, and the electron beam applicator and frame of $15 \times 15 \text{ cm}^2$, as described before. Moreover, we measured and applied the correction factors for the effect of a change in polarity applied to the chamber (k_{pol}), lack of complete charge collection (k_s), electrometer calibration factor (k_{elec}), and differences of temperature and pressure between the standard laboratory and our facility at the time of the measurements (k_{TP}) to the charge values obtained. Each measurement was performed three times in the same day, and we employed the mean value for the analysis ($n = 3$). We repeated this measurement procedure four times along four months ($n = 4$), varying the operating medical physicist ($n = 3$).

After collecting the values, we applied different formalisms (evaluated protocols) for the determination of the absorbed dose rate to water ($D_{w,Q}$) at the depth of maximum dose (z_{max}) for each electron beam quality (Q), as described in the following sections.

2.1. TRS-398 formalism (standard and adapted)

Here we employed the TRS-398 protocol using a parallel-plate P11 chamber (TRS-398 (pp)) as the reference protocol. Thus, the values of absorbed dose to water determined by the TRS-398 (pp) protocol are represented here by $D_{w,Q}(\text{ref})$. Other protocol results of $D_{w,Q}$ are generically represented by $D_{w,Q}(\text{eval})$, and were compared with the $D_{w,Q}(\text{ref})$'s results.

For the standard TRS-398 protocol, we cross-calibrated the P11 chamber against the A12 using the higher energy electron beam (15 MeV – $R_{50} = 6.42 \text{ g.cm}^{-2}$). The cross-calibration procedure was carried out following the protocol recommendations [1]. Briefly, we positioned the center of the A12 chamber at $z_{\text{ref}} + 0.5r_{\text{cav}}$ for the 15 MeV beam and measured the correction factors and the collection charge. After that, we positioned the P11 chamber at z_{ref} discounting 1 mm of the front wall (as described before) and measured the correction factors and collection charge. We applied the equations presented in the protocol (for more information, please see chapter 7, section 7.6 of the ref. [1]) and were able to determine the calibration factor in terms of absorbed dose to water ($N_{D,w,Q_{\text{cross}}}$) for the P11 chamber. With this value, we calculated the $D_{w,Q}$ [Gy] at z_{max} for each electron beam, using equation 1:

$$D_{w,Q}(z_{\text{max}}) = 100M_Q N_{D,w,Q_{\text{cross}}} k_{Q,Q_0} / PDD(z_{\text{ref}}) \quad (1)$$

Where M_Q is the measured charge [C], $N_{D,w,Q_{\text{cross}}}$ is the calibration factor [Gy/C] for the P11 chamber obtained from the cross-calibration procedure, and k_{Q,Q_0} is the quality conversion factor [dimensionless] for the P11 chamber obtained by the equation 2:

$$k_{Q,Q_0}(pp) = k_{Q,Q_{\text{int}}} / k_{Q_0,Q_{\text{int}}} \quad (2)$$

Where $k_{Q,Q_{\text{int}}}$ is the P11 quality conversion factor for the measured beam energy [dimensionless], and $k_{Q_0,Q_{\text{int}}}$ is the quality conversion factor for the 15 MeV beam. Both values were obtained using a linear interpolation of the values made available by the protocol (Table 7.IV of the ref. [1]).

As one of our objectives, we also employed the A12 cylindrical chamber to obtain the $D_{w,Q}$. Since the protocol does not present the k_{Q,Q_0} values for cylindrical chambers for $R_{50} < 4 \text{ g.cm}^{-2}$, we employed

two strategies to calculate these values. The first was to use a linear extrapolation of the available values (Table 7.III of the ref. [1]), which gave us equation 3:

$$k_{Q,Q0}(linear) = -0.0027R_{50} + 0.9306 \quad (3)$$

The second was to employ a power fitting function to the available values since previous data suggests that the curve profile is better represented by a power function [9]. This approach gave us equation 4:

$$k_{Q,Q0}(power) = 0.9613R_{50}^{-0.028} \quad (4)$$

Using these two strategies, we calculated the $D_{w,Q}$ at z_{max} , using equation 5:

$$D_{w,Q}(z_{max}) = 100M_Q(z_{ref} + 0.5r_{cav})N_{D,w,Q0}k_{Q,Q0}/PDD(z_{ref}) \quad (5)$$

$N_{D,w,Q0}$ is the calibration factor for the A12 chamber obtained from direct calibration in ^{60}Co beam by the Calibration Laboratory of the Nuclear and Energy Research Institute (IPEN – São Paulo, Brazil).

2.2. TG 51 formalism

Although the TG 51 protocol does not recommend employing a cylindrical chamber for electron beam dosimetry when $R_{50} < 2.6 \text{ g.cm}^{-2}$, it made available the equations to obtain the quality conversion factors for all energies of electron beams [2]. In this case, the quality conversion factor is factored in two: the photon-electron conversion factor (k_{ecal} [dimensionless]) and the quality conversion factor (k'_{R50} [dimensionless]). The first is a constant value fixed for a chamber model, which the literature presents slightly different values (obtained from experimental measurements or using MC simulations). An exponential function represents the second, and in the case of any cylindrical chamber, it is equation 6:

$$k'_{R50}(cyl) = 0.9905 + 0.710e^{(-R50/3.67)} \quad (6)$$

In the TG 51 protocol, the chamber is positioned with its central axis at z_{ref} , and the protocol also recommends using a gradient correction factor (P_{gr} [dimensionless]), which can be obtained using equation 7:

$$P_{gr} = \frac{M(z_{ref}+0.5r_{cav})}{M(z_{ref})} \quad (7)$$

Furthermore, we employed two different values of k_{ecal} available in the literature for the A12 Exradin chamber: the original value made available by the protocol (TG-51a - $k_{ecal} = 0.906$), and the value calculated by Muir and Rogers in 2014 using MC simulations (TG-51b - $k_{ecal} = 0.912$) [9].

Therefore, the $D_{w,Q}$ at z_{max} could be calculated using equation 8:

$$D_{w,Q}(z_{max}) = 100M_Q N_{D,w,Q0} P_{gr} k_{ecal} k'_{R50} / PDD(z_{ref}) \quad (8)$$

2.3. Muir 2020 formalism

In 2020, Muir proposed a new formalism for electron beam reference dosimetry based on MC simulations [11]. Here, the quality conversion factor is also factored in two: k'_Q and $k_{Q,ecal}$ [dimensionless]. The factors are very similar to the TG 51 formalism, with the difference of k'_Q being represented by a specific equation for each chamber model, which already includes the P_{gr} value. For the A12 chamber model, the k'_Q can be calculated using equation 9:

$$k'_Q(A12) = 0.965 + 0.119R_{50}^{-0.607} \quad (9)$$

And the $D_{w,Q}$ at z_{max} can be calculated using equation 10:

$$D_{w,Q}(z_{max}) = 100M_Q N_{D,w,Q0} k_{Q,ecal} k'_Q / PDD(z_{ref}) \quad (10)$$

2.4. Analysis of k_Q values for the A12 cylindrical chamber

Using the values of dose obtained by each protocol and employing the equations 3, 4, 5, 8, and 9, we were able to calculate the ideal k_Q values so that $D_{w,Q}(eval)/D_{w,Q}(ref)=1$ (i.e., the k_Q values that would make the results of each studied protocol equal the TRS-398 results). In this analysis, our k_Q

notation represents a conversion factor that includes every conversion factor term described by each protocol. Therefore, for the TRS-398 (linear) and (power) approaches the k_Q notation represents the ideal $k_{Q,Q0}$ values, while for the TG 51 it is the product of k_{ecal} and k'_{R50} , and for the Muir's formalism, it is the product of $k_{Q,ecal}$ and k'_Q . The calculated k_Q values ($k_Q(calc)$) were compared with the k_Q values provided by the protocols ($k_Q(prov)$).

2.5. Analysis and statistics

The results are expressed as the ratio of the absorbed dose rate to water obtained from the evaluated protocols ($D_{w,Q(eval)}$) by the absorbed dose rate to water obtained from the reference protocol ($D_{w,Q(ref)}$). In the case of the k_Q analysis (item 2.4), we also presented the results as the ratio between the conversion factors calculated by those provided by each protocol ($k_Q(calc)/k_Q(prov)$). The data are also discussed in terms of relative percentage differences (equation 11):

$$Diff(\%) = \frac{|D_{w,Q(ref)} - D_{w,Q(eval)}|}{D_{w,Q(ref)}} 100 \quad (11)$$

The repeated data are presented in the graphs as a mean \pm standard deviation of the measurements carried out over four months ($n=4$) and by different medical physicists ($n=3$).

3. RESULTS AND DISCUSSION

We determined the R_{50} , Z_{ref} , and PDD values at Z_{ref} values from the PDD curves obtained. These values are presented in Table 1.

Table 1: Beam parameters determined from the PDD curves data

	Nominal Energy (MeV)				
	4	6	9	12	15
R_{50} (g.cm ⁻²)	1.23	2.33	3.64	5.09	6.42
Z_{ref} (g.cm ⁻²)	0.64	1.30	2.09	2.95	3.75
PDD at Z_{ref} (%)	100	100	100	99.9	99.5

The values presented in Table 1 were determined using the TRS-398 formalism [1]. The data showed a good agreement with the last LINAC commissioning data available in the department

(2011), where the values differed less than 0.05 g.cm^{-2} from the commissioning data (data not shown). This agreement shows the reliability of both the LINAC and the ionization chamber.

Figure 1 shows the values of $D_{w,Q}(\text{eval})/D_{w,Q}(\text{ref})$ obtained for all protocols evaluated. As commented before, for the TG 51 data, we utilized two different values for k_{ecal} : the original value made available by the protocol (TG-51a - $k_{\text{ecal}} = 0.906$), and the value calculated by Muir and Rogers in 2014 [9], using MC simulations (TG-51b - $k_{\text{ecal}} = 0.912$).

Figure 1: Values of $D_{w,Q}(\text{eval})/D_{w,Q}(\text{ref})$ obtained for all protocols evaluated. Closed circles: TG-51a/TRS-398(pp); open circles: TG-51b/TRS-398(pp); triangles: Muir, 2020/TRS-398(pp); closed diamonds: TRS-398(linear) /TRS-398(pp); and open diamonds: TRS-398(power) / TRS-398(pp).

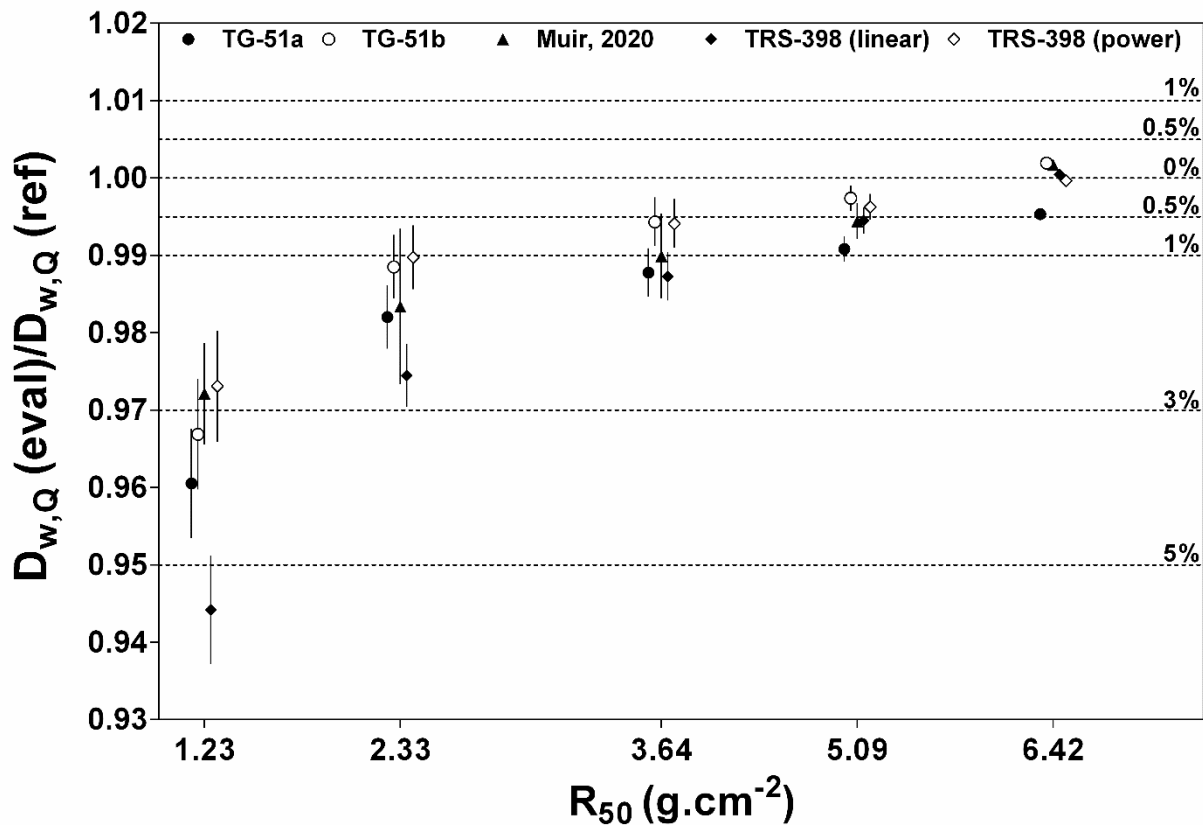


Fig.1 compares the evaluated values with those from the reference protocols (TRS-398 (pp)). As expected, the comparisons between the TRS-398 (linear) using the A12 chamber and the TRS-398 (pp) showed the biggest ratio values for the low-energy electron beams. When using cylindrical chambers for beams with $R_{50} \geq 4 \text{ g.cm}^{-2}$, the protocol recommends linear interpolating $k_{Q,Q0}$ data to

determine the values for a specific R_{50} value [1]. However, this approach was expected to show the worst results for beams with $R_{50} < 4 \text{ g.cm}^{-2}$, mainly because the profile of the k_{Q,Q_0} tends to a power function rather than a linear function (especially in low energy beams) [9]. Still, we evaluated this approach because of its convenient simplicity and quickness in the case of the unavailability of a parallel-plate chamber in a department that follows the TRS-398 formalism. In this way, if a linear approach is employed to estimate the k_{Q,Q_0} values from the TRS-398 data, our results show an expected mean difference of around 5.5% from the standard methodology for the 4 MeV beam (R_{50} of 1.23 g.cm^{-2}). When using a power fitting function (TRS-398(power)), the ratios dramatically decrease, reaching lower differences than other protocols for most energies. These results show that in the case of the unavailability of a parallel-plate chamber, one can get acceptable differences (less than 3% [12]) for low-energy electron beams using a power fitting function to determine the k_{Q,Q_0} values from the TRS-398 data.

The results for the 4 MeV beam using the TG 51 protocols showed mean differences of 4 and 3.3% for the TG 51a (k_{ecal} from TG 51), and TG 51b (k_{ecal} from ref. [9]), respectively. It is worth pointing out that when using the more recent k_{ecal} value, obtained by Muir and Rogers using MC simulations (TG 51b), the differences are lower than when using the TG 51 data (TG 51a), which can be related to the systematic uncertainties in the data presented by the TG 51 protocol [9]. Still, when using both TG 51a and b, the values differ more than the power fitting function. Although the comparisons made here are based on different types of chambers (TG 51: cylindrical; TRS-398: parallel-plate), both TG 51 and TRS-398 are from the same era, and their data were obtained employing similar techniques and methodologies, that is, the differences found may be related to uncertainties from both protocols and both chamber types.

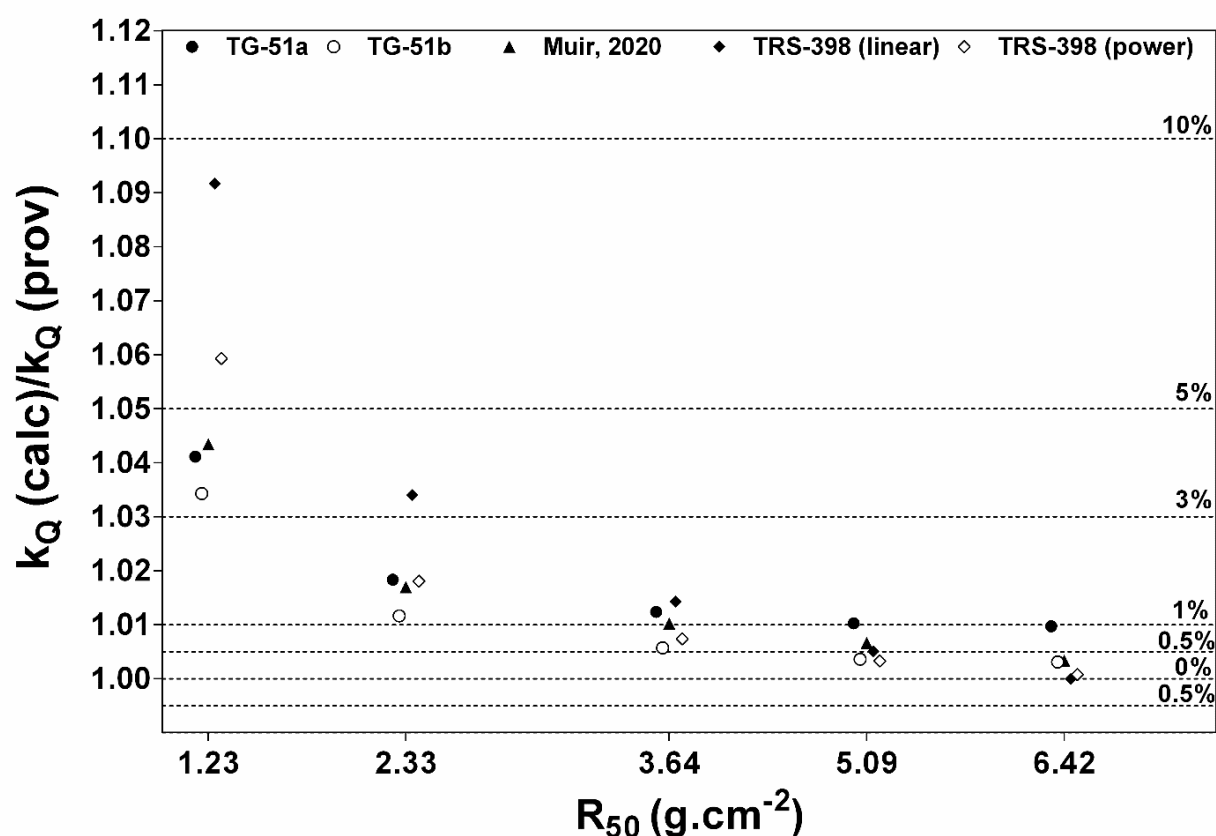
Evaluating the Muir, 2020 protocol, we found mean differences of 2.7 and 1.8% for the 4 MeV (R_{50} of 1.23 g.cm^{-2}) and 6 MeV (R_{50} of 2.33 g.cm^{-2}) beams respectively [11]. As the power fitting approach, these data are in the acceptable differences range. Furthermore, this is the most recent protocol, where its data were obtained using more recent and sophisticated methods. Compared with the TG 51 procedure, Muir's protocol claims not to need P_{gr} correction factor, which would simplify the process and make it more straightforward.

Here, we employed the parallel plate chamber (discounting its front wall – 1.0 mm) for the PDD measurements, which is equivalent to use a cylindrical chamber with a shift of $0.5r_{\text{cav}}$ (1.53 mm –

A12), as described in the TRS-398 and TG 51 protocols. We employed this methodology for all protocols with the purpose of standardization of the measurements procedure and R_{50} determination. However, it is important to mention that Muir's protocol suggests that the effective point of measurement vary with the chamber type. In the case of an Exradin A12 chamber, the Muir's papers suggest using an optimal shift of $0.35r_{cav}$ (1.07 mm) for the PDD measurements, which is equivalent to a shift of 1.4 mm for the P11 parallel plate chamber. Using these recommended shift values, it would result in slight different values of R_{50} , what may perhaps improve the results found here [9,11].

Fig.2 presents the ratio between the calculated k_Q values and the ones from the protocols provided.

Figure 2: Values of $k_Q(\text{calc})/k_Q(\text{prov})$ obtained. Closed circles: TG-51a/TRS-398(pp); open circles: TG-51b/TRS-398(pp); triangles: Muir, 2020/TRS-398(pp); closed diamonds: TRS-398(linear) /TRS-398(pp); and open diamonds: TRS-398(power) / TRS-398(pp).



The ideal values of k_Q were calculated (data not shown) to achieve the same dose values as the TRS-398 protocol when employing the other protocols. Thus, it is possible to utilize these values to

calculate the absorbed dose to water using the A12 chamber and any of the evaluated protocols, achieving the same values as those of TRS-398. Note that these values were calculated in specific conditions, using a particular ionization chamber and LINAC.

From the Figs. 1 and 2 data, we realized that the differences found were similar to the magnitude of the P_{gr} values (i.e., $M_Q(z_{ref}+0.5r_{cav})/M_Q(z_{ref})$). Therefore, we recalculated the $D_{w,Q}(eval)$ values using $M_Q(z_{ref}+0.5r_{cav})$ instead of $M_Q(z_{ref})$, for both the TG 51 and the Muir, 2020 protocols. Fig. 3 shows the values of $D_{w,Q}(eval)/D_{w,Q}(ref)$ obtained for all protocols evaluated, substituting the $M_Q(z_{ref})$ values by the $M_Q(z_{ref}+0.5r_{cav})$ in the case of TG 51 and Muir, 2020 protocols.

Figure 3: Values recalculated of $D_{w,Q}(eval)/D_{w,Q}(ref)$ obtained substituting the $M_Q(z_{ref})$ values by the $M_Q(z_{ref}+0.5r_{cav})$. Closed circles: TG-51a/TRS-398(pp); open circles: TG-51b/TRS-398(pp); triangles: Muir, 2020/TRS-398(pp); closed diamonds: TRS-398(linear) /TRS-398(pp); and open diamonds: TRS-398(power)/ TRS-398(pp).

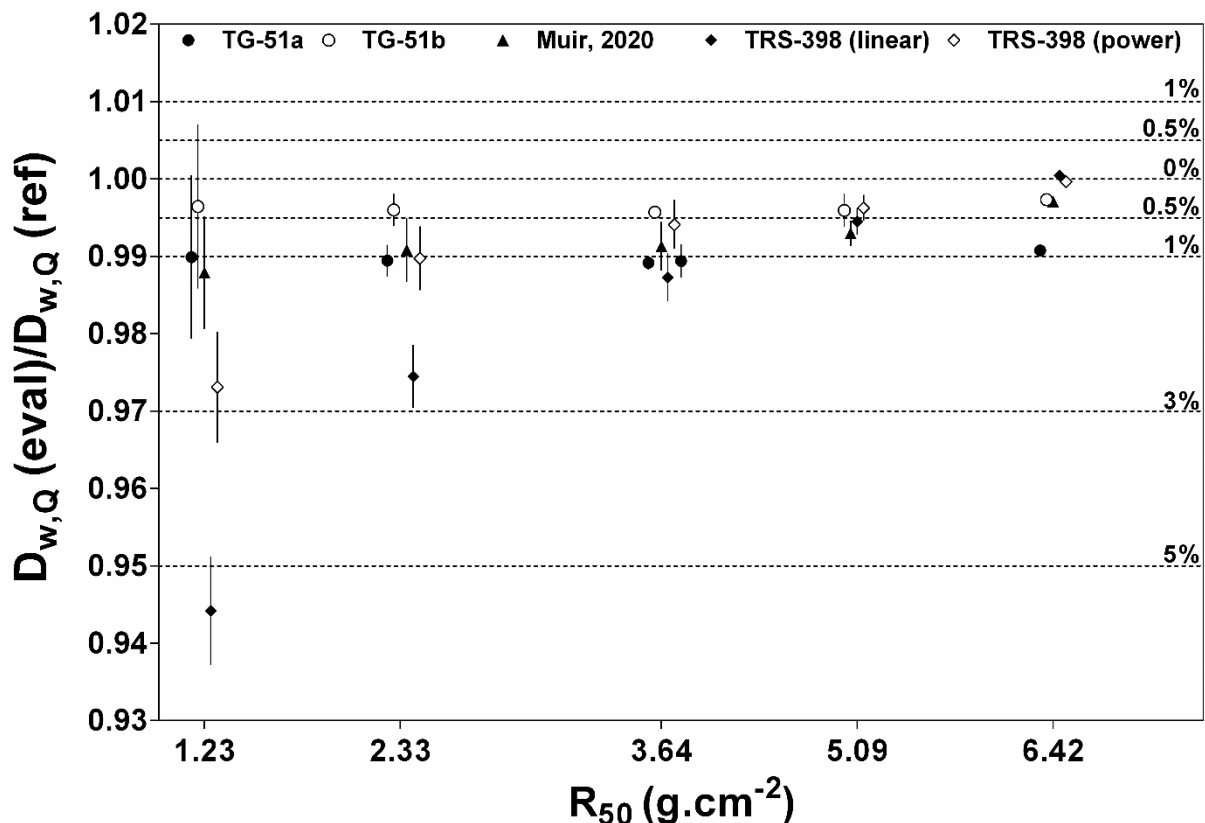


Fig. 3 shows the results using the values of collected charge with a shift of $0.5r_{\text{cav}}$ of the A12 chamber's central axis. It is important to note that the TRS-398 protocol recommends using the $0.5r_{\text{cav}}$ shift when cylindrical chambers are employed for cross-calibration of parallel-plate chambers, while other protocols do not [2, 11]. However, when using the values with the shift, the differences between both protocols (TG 51 and Muir, 2020) and the TRS-398 decreased. Analyzing the results for the lower beam energies, i.e., 4, 6, and 9 MeV beams (R_{50} of 1.23, 2.33, and 3.64 g.cm⁻²), the results for TG 51a and b showed differences of around 1 and 0.4%, respectively. The results obtained by TRS-398 (linear) and (power) maintained the same results as presented in Fig.1 since the methods originally employed the values of $M_Q(z_{\text{ref}}+0.5r_{\text{cav}})$ for dose calculation (as described in section 2.1.). When applying the $M_Q(z_{\text{ref}}+0.5r_{\text{cav}})$ values in the Muir, 2020 protocol, we found a difference of 1.2% for the 4 MeV beam and lower values when increasing the beam energy. Moreover, when using the Muir, 2020 protocol, there is no need to use P_{gr} corrections for dose calculation, making the procedure simpler and faster. In this way, this protocol shows the best cost-benefit profile for electron beam dosimetry (with or without the use of the chamber shifting), as suggested before [5, 9, 11].

4. CONCLUSION

Here we presented the comparison between using a parallel-plate P11 chamber with the TRS-398 formalism and a cylindrical A12 chamber using different protocols for electron beam dosimetry. In our case, we present data regarding using an A12 ionization chamber with both wall and electrode made of C-552. Previous studies already commented on their use but showed data only about a chamber with a wall made of graphite and electrodes made of aluminum (NE2571) [5]. Some evaluated protocols showed differences below 3% compared to the TRS-398 (pp) protocol, whereas the Muir, B.R. 2020 protocol showed the best cost-benefit relationship. Therefore, our data can bring confidence in using a cylindrical chamber in the case of unavailability of a parallel-plate chamber or in the case of new protocols implementation (and addendums to the former protocols) that allow the use of cylindrical chamber for electron beam reference dosimetry.

Once again, it is of paramount importance to highlight that the TRS-398 data, and the use of parallel-plate ionization chambers, present some intrinsic uncertainties [5, 9, 11], which may have

influenced our result (since we analyzed the ratio between the results of the evaluated protocols by the TRS-398 results). Thus, future works can employ more sophisticated and precise dosimetry methodologies (such as calorimetric, Fricke, and others) to evaluate the use of cylindrical chambers and different protocols for low-energy electron beam reference dosimetry.

ACKNOWLEDGMENT

We thank the Medical Physics core, and the Multi-professional residence program, in special the Medical Physics residence coordination. We also thank the Ministry of Health of Brazil for the residence fellowship.

REFERENCES

- [1] IAEA (INTERNATIONAL ATOMIC ENERGY AGENCY) – Technical Report Series 398: Absorbed Dose Determination in External Beam Radiotherapy, Vienna: **INTERNATIONAL ATOMIC ENERGY AGENCY**, 2001. Available at: <<https://www.iaea.org/publications/5954/absorbed-dose-determination-in-external-beam-radiotherapy>>. Last accessed: 30 Apr. 2023.
- [2] ALMOND, P. R.; BIGGS, P J.; COURSEY, B. M.; HANSON, W. F.; HUQ, M. S.; NATH, R.; ROGERS, D. W. O. AAPM's TG-51 protocol for clinical reference dosimetry of high-energy photon and electron beams. **Med Phys**, v. 26(9), p. 1847-1870, 1999. Available at <<https://aapm.onlinelibrary.wiley.com/doi/abs/10.1118/1.598691>> . Last accessed: 30 Apr. 2023.
- [3] THWAITES, D. I.; DUSAUTOY, A.R.; JORDAN, T.; MCEWEN, M. R.; NISBET, A.; NAHUM, A. E.; PITCHFORD, W. G. The IPEM code of practice for electron dosimetry for radiotherapy beams of initial energy from 4 to 25 MeV based on an absorbed dose to water calibration. **Phys Med & Biol**, v. 48(18), p. 2929-2970, 2003. Available at:

- <<https://iopscience.iop.org/article/10.1088/0031-9155/48/18/301>>. Last accessed: 30 Apr. 2023.
- [4] WITTKAMPER, F. W.; THIERENS, H.; VAN DER PLAETSEN, A.; WAGTER, C.; MIJNHEER, B. J. Perturbation correction factors for some ionization chambers commonly applied in electron beams. **Phys Med & Biol**, v. 36(12), p. 1639-1652, 1991. Available at: <<https://iopscience.iop.org/article/10.1088/0031-9155/36/12/008>>. Last accessed: 30 Apr. 2023.
- [5] MUIR, B.R. and M.R. McEWEN. On the use of cylindrical ionization chambers for electron beam reference dosimetry. **Med Phys**, v. 44(12), p. 6641-6646, 2017. Available at: <<https://aapm.onlinelibrary.wiley.com/doi/10.1002/mp.12582>>. Last accessed: 30 Apr. 2023.
- [6] STEWART, K. and SEUNTJENS, J. Comparing calibration methods of electron beams using plane-parallel chambers with absorbed-dose to water based protocols. **Med Phys**, v. 29(3), p. 284-289, 2002. Available at: <<https://aapm.onlinelibrary.wiley.com/doi/abs/10.1118/1.1449876>>. Last accessed: 30 Apr. 2023.
- [7] ZINK, K.; CZARNECKI, S.; LOOE, H. K.; VON VOIGTS-RHETZ, P.; HARDER, D. Monte Carlo study of the depth-dependent fluence perturbation in parallel-plate ionization chambers in electron beams. **Med Phys**, v. 41(11), p. 111707, 2014. Available at: <<https://aapm.onlinelibrary.wiley.com/doi/full/10.1118/1.4897389>>. Last accessed: 30 Apr. 2023.
- [8] BUCKLEY, L.A. and ROGERS, D. W. O. Wall correction factors, for parallel-plate ionization chambers. **Med Phys**, v. 33(6Part1), p. 1788-1796, 2006. Available at: <<https://aapm.onlinelibrary.wiley.com/doi/10.1118/1.2161403>>. Last accessed: 30 Apr. 2023.
- [9] MUIR, B. R. and ROGERS, D. W. O. Monte Carlo calculations of electron beam quality conversion factors for several ion chamber types. **Med Phys**, v. 41(11), p. 111701, 2014. Available at: <<https://aapm.onlinelibrary.wiley.com/doi/full/10.1118/1.4893915>>. Last accessed: 30 Apr. 2023.
- [10] MUIR, B. R., MCEWEN, M. and ROGERS, D. W. O. Beam quality conversion factors for parallel-plate ionization chambers in MV photon beams. **Med Phys**, v. 39(3), p. 1618-1631,

2012. Available at: <<https://aapm.onlinelibrary.wiley.com/doi/full/10.1118/1.3687864>>. Last accessed: 30 Apr. 2023.

[11] MUIR, B. R. A modified formalism for electron beam reference dosimetry to improve the accuracy of linac output calibration. **Med Phys**, v. 47(5), p. 2267-2276, 2020. Available at: <<https://aapm.onlinelibrary.wiley.com/doi/full/10.1002/mp.14048>>. Last accessed: 30 Apr. 2023.

[12] INCA (INSTITUTO NACIONAL DO CANCER) TEC DOC - 1151: aspectos físicos da garantia da qualidade em radioterapia. **Programa de Qualidade em Radioterapia**, Rio de Janeiro, Brasil Ministério da Saude, 2000. Available at: <<https://www.inca.gov.br/publicacoes/notas-tecnicas/tecdoc-1151-aspectos-fisicos-da-garantia-da-qualidade-em-radioterapia>>. Last accessed: 30 Apr. 2023.

This article is licensed under a Creative Commons Attribution 4.0 International License, which permits use, sharing, adaptation, distribution and reproduction in any medium or format, as long as you give appropriate credit to the original author(s) and the source, provide a link to the Creative Commons license, and indicate if changes were made. The images or other third-party material in this article are included in the article's Creative Commons license, unless indicated otherwise in a credit line to the material.

To view a copy of this license, visit <http://creativecommons.org/licenses/by/4.0/>